Available online at www.sciencedirect.com
ScienceDirect
Materials and Design 28 (2007) 2540–2543
Materials & Design
www.elsevier.com/locate/matdes

Short Communication

Processing, microstructure and creep testing of Pt–Y_2O_3 composites

M. Besterci [a,*], P. Hvizdoš [b], K. Sülleiová [a], Ch. Edtmaier [c]

[a] Institute of Materials Research of SAS, Watsonova 47, 043 53 Košice, Slovak Republic
[b] Department of Materials Science, and Metallurgical Engineering, Polytechnic University of Catalonia, Diagonal 647, 08028-Barcelona, Spain
[c] Institut für Chemische Technologie Anorganischer Stoffe, TU Wien, Getreidemark 9/161, A-1060 Wien, Austria

Received 30 January 2006; accepted 8 September 2006
Available online 9 November 2006

Abstract

Two Pt–Y_2O_3 composites were prepared from recycled wastes by powder metallurgy technique using two different times (8 and 24 h) of low-energy mechanical alloying and their high temperature deformation behaviour was investigated by compressive creep testing at 1200 and 1573 K. The creep strain of the two materials was mutually compared and the role of the milling time was identified. The material milled for 24 h had superior creep resistance due to the better distribution of yttria particles. The microstructure of the Pt–Y_2O_3 system (material B) was analyzed by optical microscopy, transmission electron microscopy (TEM) and scanning electron microscopy (SEM).

1. Introduction

Platinum and its alloys are widely utilized in glass industry. The materials have to satisfy requirements like: chemical purity, good and reliable mechanical properties at temperatures up to 1773 K, and sufficient chemical stability without interacting with glass melt, for instance for glass furnace lining [1–4]. Dispersion strengthening methods, microstructures, properties and utilization of Pt based composites are described in these works, mainly in [3].

Stabilization of the matrix microstructure at high temperature exposure is achieved by incorporating of the secondary phase particles into the matrix. Since the Pt is expensive, in metallurgy only infrequently used material, unconventional preparation procedures, using powder metallurgy techniques, are being developed to produce Pt based composites. Here, the problems of compacting, shaping, and welding have to be addressed. The optimum system seems to be Pt–Y_2O_3 composite, whose microstructure, mechanical properties and fracture is dealt with in works [5–11]. Size and morphology of Y_2O_3 particles in the Pt–Y_2O_3 system are evaluated in [5]. Experimental results of fracture micromechanisms of Pt–Y_2O_3 composites in relation to qualitative factor are described in [6]. The work [7] deals with the evaluation of mechanical properties of Pt–Y_2O_3 materials. Edtmaier developed calibration standards for Pt–Au system [8]. Mechanical properties of composites based on Pt at elevated temperatures are described in [9,10]. The studied materials were prepared by powder metallurgy from recycled matrix Pt powder. This technology includes the two-stage reduction of Pt, low-energy mechanical alloying, hot isostatic pressing (HIP), and final compacting by rolling. Corrosion resistance of Pt in glass furnaces is the object of study in the work [11].

The aim of this work is to analyze microstructure and the creep behaviour of Pt–Y_2O_3 composite samples prepared by two ways of mechanical alloying.

2. Experimental material and methods

The materials for creep experiments were manufactured as follows. The matrix Pt powder was prepared from Pt wastes, which were first dissolved in aqua regia. From the solution the crystals of ammonium chloride were obtained by coagulation and then they were thermally decomposed to yield the Pt powder. After refining, drying, reducing, and de-gassing, the Pt powder was milled together with 0.5 mass% of Y_2O_3. Two different

* Corresponding author. Tel.: +421 55 7922111; fax: +421 55 7922408.
E-mail address: mbesterci@imr.saske.sk (M. Besterci).

0261-3069/$ - see front matter © 2006 Elsevier Ltd. All rights reserved.
doi:10.1016/j.matdes.2006.09.012

times of the milling (low-energy mechanical alloying) were used: 8 h (hereafter referred to as material A) and 24 h (hereafter referred to as material B). The milling was carried out in the mills with ZrO_2 spheres in protective Ar atmosphere. The resulting mixture was HIP-ed at 1523 K/175 MPa, and subsequently hot rolled at 1473 K.

The experimental materials were cut to bars 5 mm high with square base of 2.5 mm × 2.5 mm. Compression creep tests were carried out in ambient air at temperatures 1473 and 1573 K. Each sample was held at the testing temperature for 15 min before testing in order to stabilize and homogenize the temperature. The specimens were loaded by a dead weight system; the load did not change during the test. The change of height was measured using an inductive transducer and was recorded as a function of time.

3. Results and discussion

Microstructure of the material B was analyzed. The fine-grained Pt matrix is identified by optical microscopy. Some grains are polyedric, sized to 2 μm, some are eliptic-elongated, with a length up to 15 μm and a width of about 2 μm. Such a morphological arrangement is made mainly in the line distribution of Y_2O_3 particles. Recrystallization at low rolling temperatures results in the line distribution of fine grains. These particles supress the grain boundaries moving in the direction of sheet thickness more intensively than in the rolling direction. There are two size categories of the Y_2O_3 particles: The particles and/or clusters of particles, sized >1 μm, identified on the fracture surfaces at bigger magnifications, and the particles from 20 to 100 nm, identified by TEM as given in Fig. 1. Selective electron diffraction of a particle from Fig. 1 is shown in Fig. 2. The dispersed phase Y_2O_3 is labelled in italics [(002); (511); (513)], it is a K8 body centered cubic lattice with a lattice parameter $a = 1.058$ nm. The Pt matrix lattice is face centered cubic K12 with $a = 0.3912$ nm, and labelled in standard font [(200); (020); (220)]. The second phase distribution in the foil surface, as shown in Fig. 3, was estimated by SEM.

The nature of the testing method (large strains accompanied by geometrical changes and decreasing stress) did not allow to resolve the typical creep stages and find the secondary (steady-state) creep rates. During the tests only decreasing of the creep rate could be observed. Particularly at higher stresses, the materials suffered very rapid deformation in the beginning of the test, probably happening completely in the primary creep regime. Then, already at considerably lower true stress levels, the creep rates decreased dramatically, so much that at 1573 K they became similar regardless of the test conditions. Nevertheless, the following useful information was obtained by comparing the results for two sample materials.

Primarily, both materials were loaded in such a way, that the initial nominal stresses were 2 and 5 MPa. The creep strain vs. time curves for both materials are shown and compared in Figs. 4 and 5. The material B exhibited consistently better high temperature deformation resistance than the material A and this tendency was retained during the whole tests. At the lower compression load (2 MPa) the material A typically suffered strains about twice as high as the material B. Higher loads led to very large strains, rapidly lowering the real stress values, which resulted in slightly lower difference between the two materials, particularly at 1573 K. Here the deformation of the material A

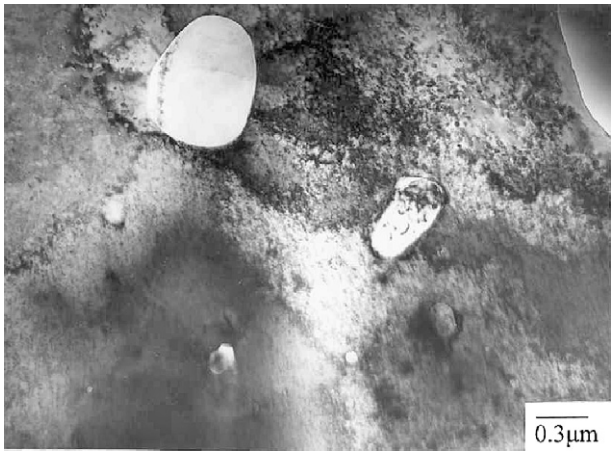

Fig. 1. Size and shape of Y_2O_3 particles.

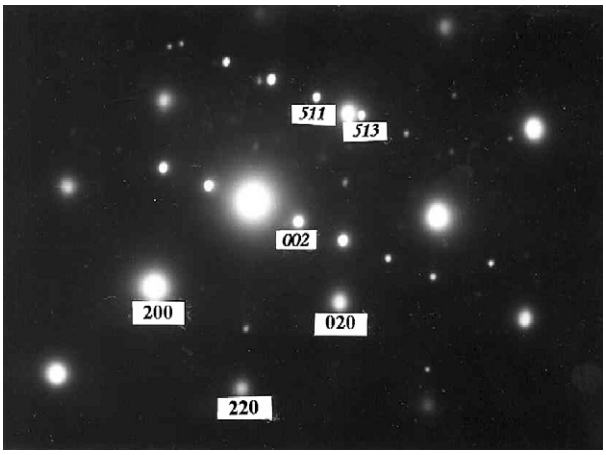

Fig. 2. Selective electron diffraction of the matrix and Y_2O_3 particles.

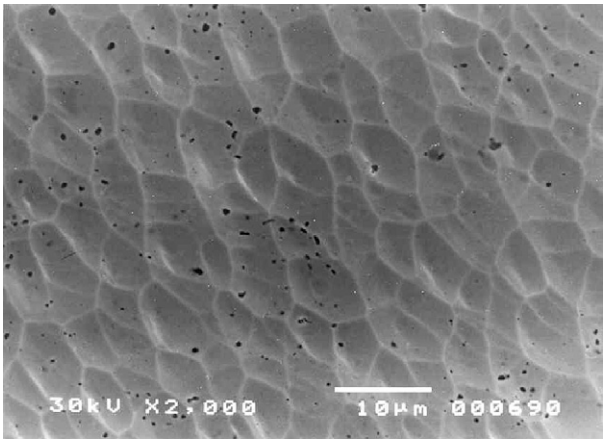

Fig. 3. Foil surface example, used for subgrain size and distribution by SEM.

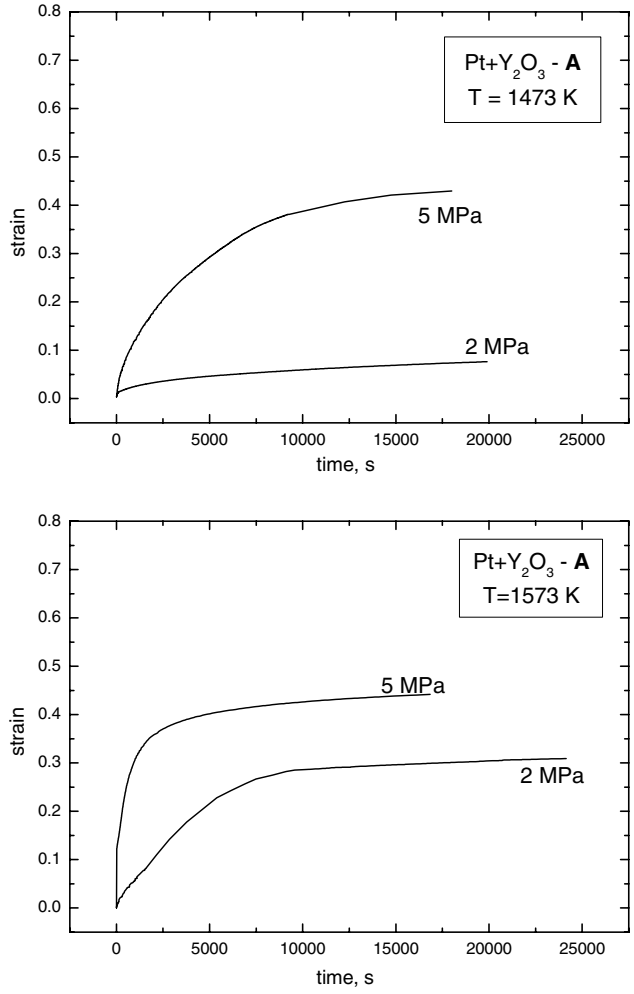

Fig. 4. Creep curves of the material A.

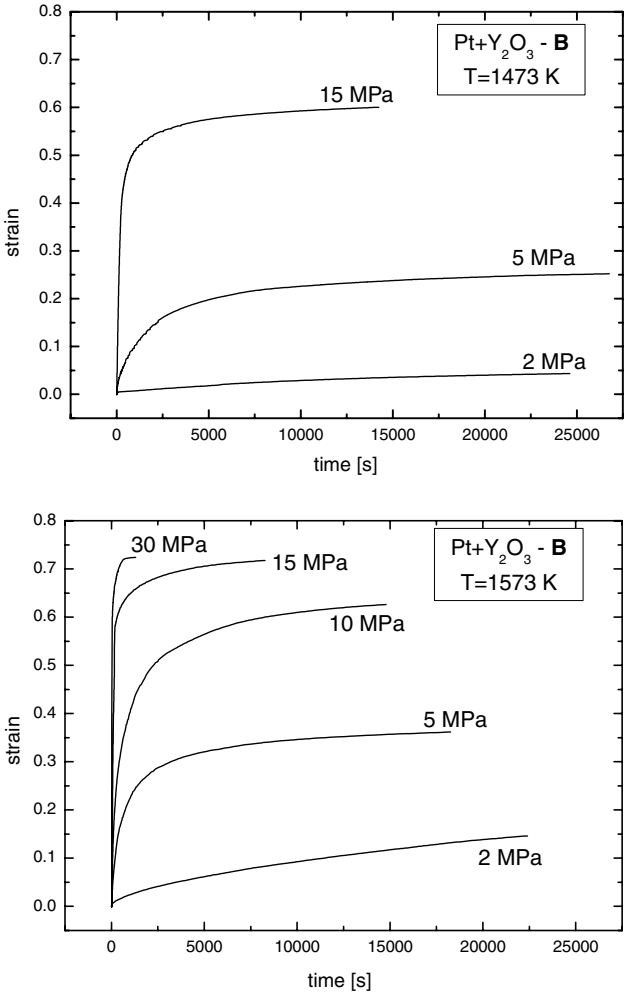

Fig. 5. Creep curves of the material B.

was higher by factor of ~1.4 than that of the material B. Generally, the higher creep resistance of the material B can be attributed to the better distribution of Y_2O_3 particles as a result of longer milling.

In order to characterize the more resistant material (material B) in greater details, it was also tested at the initial load of 15 MPa (1473 and 1573 K), as well as at 10 and 30 MPa (1573 K). The results can be seen in Fig. 2. At 1573 K the strain in the test with the initial load of 15 MPa reached 71% after 2 h, and at 30 MPa the same strain level was reached after 10 min.

The strain rates ($\dot{\varepsilon}$) at a specific level of strain ($\varepsilon = 0.1$) were calculated for quantitatively describing the deformation process of both materials in the absence of the secondary creep data. This strain was chosen because at this stage the geometry of the samples did not change significantly and also because it was possible to compare the experiments done under all testing conditions. Assuming a simple Norton–Arrhenius law

$$\dot{\varepsilon} = A\sigma^n \exp(-Q/RT), \quad (1)$$

where A is a constant, σ is the stress, n is stress exponent, Q is activation energy, R is the universal gas constant, and T is the temperature, the stress exponent can be found from a log–log plot of the strain rate ($\dot{\varepsilon}$) vs. stress (σ). The corresponding plot is shown in Fig. 6. Both materials showed

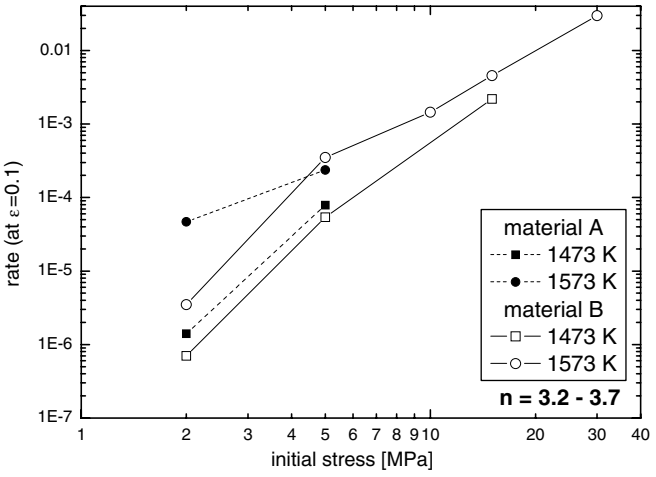

Fig. 6. The creep rates at $\varepsilon = 0.1$ as functions of stress at the test temperatures.

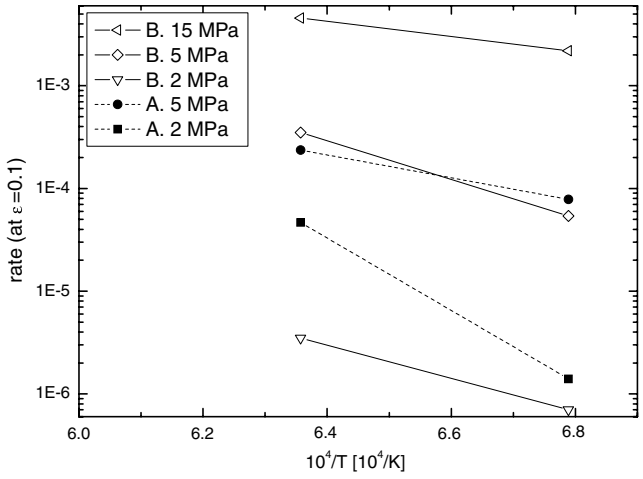

Fig. 7. The creep rates at $\varepsilon = 0.1$ as functions of temperatures at the testing stresses.

Table 1
Apparent activation energies for $\varepsilon = 0.1$ obtained in this work

Sample	Initial load (MPa)	Activation energy ($\varepsilon = 0.1$) (kJ/mol)
Material A	2	670
	5	211
Material B	2	308
	5	357
	15	141

a very similar creep behaviour in all cases and the values of the n were in the range from 3.2 to 3.7.

Using the Arrhenian type temperature dependence (see Eq. (1)), the apparent activation energies at the $\varepsilon = 0.1$ can be calculated from the log $\dot{\varepsilon}$ vs. $1/T$ plot (see Fig. 7). The results are given in the Table 1. It should be, however, mentioned that some reservation have been stressed regarding the quantitative accuracy of these activation energy values, because of the scarcity of the experimental data at two temperatures only.

4. Conclusions

1. The fine grained Pt matrix was identified by light microscopy. Some grains are polyedric, sized to 2 μm, some are elongated with a length of 15 μm and a width of 2 μm. The Pt–Y_2O_3 particles and/or clusters of particles, sized >1 μm, identified on the fracture surface, and the particles from 20 to 100 nm, identified by transmission electron microscopy.
2. Two Pt–Y_2O_3 composites were prepared from recycled Pt wastes using powder metallurgy procedures and mechanical alloying. Two different milling times were applied. The high temperature deformation resistance of the experimental materials was characterized by means of compressive creep and the role of the milling time has been investigated. The creep strain of the material milled for 24 h was usually about half of the strain of the other material under the same condition. This superior creep resistance of the former was attributed to the better distribution of Y_2O_3 particles.

Acknowledgements

The work was supported by the Slovak Grant Agency under the project no. 2/5142/25 and by the Ministry of Science and Technology of Spain through the ''Ramón y Cajal Programme'' (stay of Pavol Hvizdoš).

References

[1] McGrath RB, Badcock GC. New dispersion strengthened platinum alloy. Platinum Metals Rev 1987;31:8.
[2] Stokes J. Platinum in the glass industry. ZGS materials supplement conventional alloys. Platinum Metals Rev 1987;31:54.
[3] Drost E. Dispersionsverfestige Platin Werkstoffe 1986;11:248.
[4] Selman GL, Day JG, Bourne AA. Dispersion strengthened platinum. Properties and characteristics of a new high temperature material. Platinum Metals Rev 1974;18:46.
[5] Besterci M, Šlesár M, Kováč L, Ivan J, Zbiral J, Edtmaier Ch. Distribution of Y_2O_3 particles in the Pt–Y_2O_3 system. J Mater Sci Lett 2000;19:151.
[6] Šlesár M, Besterci M, Sülleiová K, Zbiral J. Effect of microstructure on mechanical properties and fracture of dispersion strengthened platinum. Metallic Mater 1999;37:73.
[7] Sülleiová K, Šlesár M, Besterci M, Zbiral J. Mechanical properties and fracture of dispersion strengthened Pt–Y_2O_3 materials. Acta Metall Slovaca 2001;7:135.
[8] Edtmaier Ch, Lehrner P, Zbiral J, Disam J. Bulk calibration standards by powder metallurgy for ICP-AES-Analysis. PM World Congress 1998:427.
[9] Besterci M, Šlesár M, Sülleiová K, Zbiral J. Gefügecharakteristik des Werkstoffes Pt–Y_2O_3. Prakt Metallogr 1997;34:246.
[10] Besterci M, Šlesár M, Sülleiová K, Ivan J, Zbiral J. Microstructure, mechanical properties and fracture of Pt–Y_2O_3 composites. High Temp Mat Proc 2005;24(1):79.
[11] Fischer B, Helmich R. Zur Korrosion von Platin durch Phosphatglas. Neue Hütte 1980;25:269.